

# Bioactivity of metallic biomaterials with anatase layers deposited in acidic titanium tetrafluoride solution

JIN-MING WU

*Department of Materials Science and Engineering, Zhejiang University, Hangzhou 310027, People's Republic of China*

FAN XIAO, SATOSHI HAYAKAWA\*, KANJI TSURU, SHINJI TAKEMOTO, AKIYOSHI OSAKA

*Biomaterials Laboratory, Faculty of Engineering, Okayama University, Tsushima, Okayama-shi, 700-8530, Japan*

*E-mail: satoshi@cc.okayama-u.ac.jp*

A simple and versatile treatment was developed to provide various metallic biomaterials such as Ti, NiTi, Ta and SUS 316L stainless steel with *in vitro* bioactivity or ability to deposit carbonate-incorporated apatite in a simulated body fluid (Kokubo solution). A well-crystallized anatase layer deposited on the metallic biomaterials surfaces after soaking them at 60 °C for 24 h in an aqueous solution of titanium tetrafluoride (40 mM) whose pH was adjusted to 1.9 with HCl. The as-coated anatase layers did not deposit apatite. When heated at 300 °C they were so bioactive as to deposit apatite within 5 day(s) in the Kokubo solution. The trace amount of fluorine weakly bound in the as-coated anatase layers was suggested to be one of the factors that suppressed the bioactivity.

© 2003 Kluwer Academic Publishers

## 1. Introduction

Metallic biomaterials such as titanium and its alloys, Ni–Ti alloys, tantalum, stainless steel and Co–Cr–Mo alloys are widely used as surgical implants for orthopedic and dental systems due to their high fracture toughness, long fatigue life, good biocompatibility, and excellent workability [1,2]. The orthopedic implants that are fixed earlier to the surrounding bone or tissue are always favorable [3,4]. Bone cement fixation is one of the current major techniques though it suffers from many problems like long-term degradation [5]. The so-called bioactive fixation, a kind of cement-less fixation, has also attracted much attention. It defines “interfacial bonding of an implant to tissue by means of formation of a biologically active hydroxyapatite layer on the implant surface” after Hench [5]. Thus, the key to the bioactive fixation is the ability of implants to form a layer of hydroxyapatite when implanted in the body. Unfortunately, as Takatsuka *et al.* [6] pointed out, none of the metallic biomaterials meets the requirement. Therefore, plasma spraying [7–9] and sputtering [10,11] have been applied to coat the implants with bioactive glasses, glass–ceramics, and calcium phosphate ceramics. Since the substrates are exposed to high temperatures in those coating processes, several disadvantages are reported [12]. Recently, Wei *et al.* [13] applied electrophoresis to coat hydroxyapatite on Ti, Ti–

6Al–4V and 316L stainless steel (SUS 316L) substrates. Their procedure was of multi-steps involving the dual coating process to prevent the layers from cracking as well as the sintering process at 875–1000 °C to obtain the desired adhesion.

An alternative is to provide the metallic biomaterials with bioactivity through chemical treatments. The following two approaches were so far most successful for titanium and its alloys: the treatments with sodium hydroxide [4, 12] and hydrogen peroxide [14] solutions followed by heat treatments at moderate temperatures. Recently, Miyazaki *et al.* [15, 16] found that the former treatment was also applicable to Ta. Unfortunately, Miyazaki *et al.* [4] and Kim *et al.* [12] confessed that the alkali approach could not be applied to NiTi, SUS 316L or Co–Cr–Mo alloy.

Kokubo's simulated body fluid (SBF) or an aqueous solution containing the same inorganic ions as the human blood plasma in similar concentrations has been used widely to examine *in vivo* bioactivity [17]. Several studies showed that anatase derived by heating amorphous titania gels was more likely to induce apatite deposition in SBF than rutile derived by heating the amorphous titania as well [12, 14–18]. Thus, the sol–gel route seems promising to develop an anatase layer on the metal substrates: the amorphous titania layer was derived from titanium alkoxides [19,20] and subsequently

\*Author to whom all correspondence should be addressed.

transformed by heating into the bioactive anatase layer. Unfortunately, it is not easy to control the hydrolysis of the alkoxides and polycondensation of the hydrated titanium species [19–23].

In the present experiment, we deposited anatase layers on the titanium, NiTi alloy, tantalum, and SUS 316L substrates in an acidic titanium tetrafluoride solution. The bioactivity of those metal substrates after such simple treatment was evaluated using SBF.

## 2. Experimental procedure

The titanium tetrafluoride solution was prepared after Shimizu *et al.* [23]. Aqueous solutions were prepared and employed unless otherwise described. Appropriate amount of reagent grade  $\text{TiF}_4$  (Nacalai Tesque Inc., Kyoto, Japan) was dissolved into an HCl solution (1.9 in pH) to yield 40 mM  $\text{TiF}_4$  solution. The Ti, NiTi, Ta and SUS316L substrates ( $1 \times 1 \times 0.1 \text{ cm}^3$  in size) were soaked in 0.1 M nitric acid, and subsequently rinsed with ethanol and distilled water. Three pieces of each metal were soaked in 20 ml of the  $\text{TiF}_4$  solution held in 50 ml-polyethylene bottles with tight screw caps, and kept in an oven at  $60^\circ\text{C}$  for 24 h. After soaking, they were rinsed gently with distilled water to detach the loosely attached particles. After drying at  $60^\circ\text{C}$  overnight, they were heat-treated at  $300^\circ\text{C}$  for 1 h in air.

SBF was prepared and pH was adjusted to 7.4 at  $36.5^\circ\text{C}$  as described in the literature [17]. The ion composition was 142.0:  $\text{Na}^+$ , 5.0:  $\text{K}^+$ , 2.5:  $\text{Ca}^{2+}$ , 1.5:  $\text{Mg}^{2+}$ , 148.8:  $\text{Cl}^-$ , 4.2:  $\text{HCO}_3^-$ , 1.0:  $\text{HPO}_4^{2-}$ , 0.5:  $\text{SO}_4^{2-}$ . The samples were autoclaved at  $121^\circ\text{C}$  for 20 min and then soaked in SBF at  $36.5^\circ\text{C}$  up to 5 d. Surface analysis was conducted using thin-film X-ray diffraction (TF-XRD, RAD IIA, Rigaku, Japan), Fourier transform infrared reflection (FT-IR, JASCO FT-IR300, Japan) spectroscopy, scanning electron microscopy (SEM, JEOL JSM-6300, Japan), and energy dispersive X-ray spectroscopy (EDS). In addition, X-ray photoelectron spectra (XPS) were measured under an ultra high vacuum ( $\sim 9 \times 10^{-10}$  Torr) using an ESCA spectrometer (S-Probe ESCA SSX-100S, Fisons Instruments, USA) and a monochromatized Al-K $\alpha$  X-ray (1486.8 eV) irradiation. The binding energy was presented in eV ( $= 1.60 \times 10^{-19}$  J) by convention and was normalized to the C 1s energy (284.46 eV) for adventitious hydrocarbons as the indirect standard.

## 3. Results

Fig. 1 shows the TF-XRD patterns of the substrates after soaking in the  $\text{TiF}_4$  solution at  $60^\circ\text{C}$  for 24 h and ultrasonic rinsing. All the profiles had sharp diffractions of anatase besides the diffractions of the metal substrates, indicating that anatase with good crystallinity was deposited on the substrates. Typical morphology of the anatase layer was illustrated in Fig. 2 for the Ta substrate. The layers on the Ti, NiTi and SUS 316L substrates had a similar microstructure. Fig. 2(a) shows anatase particles with sizes of about  $1 \mu\text{m}$ . Fig. 2(b) shows that they were actually the aggregates of primary anatase particles with sizes of several tens of nanometers. Such aggregation gave a porous microstructure. Fig. 2(c) indicates the

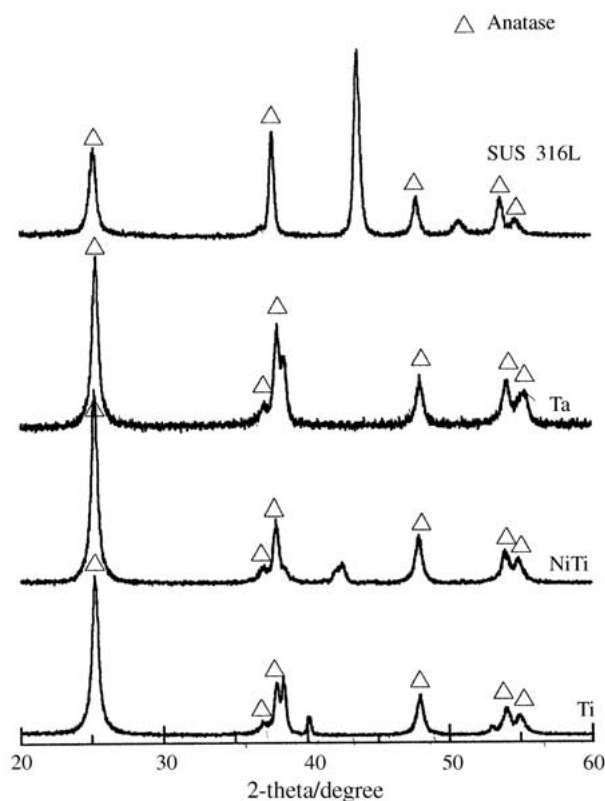


Figure 1 The TF-XRD patterns of Ti, NiTi, Ta and SUS 316L substrates treated with the  $\text{TiF}_4$  solution at  $60^\circ\text{C}$  for 24 h. The diffractions without any symbols were from the substrates.

presence of a solid layer under the porous layer: both were durable to the ultrasonic cleaning for up to 5 min. From Fig. 1 it is clear that the solid layer also consisted of anatase. The EDX analysis of the layer on the Ta substrates naturally indicated the presence of no other elements than Ti, Ta, and O.

None of the as-coated substrates deposit apatite even after 10 d in SBF. Thus, they were heated at  $300^\circ\text{C}$  for 1 h in air and subsequently soaked in SBF for only 5 d. Then, the TF-XRD profiles of the Ti, Ta and SUS 316L substrates in Fig. 3 showed strong diffractions assignable to apatite, though NiTi had weaker diffractions. The broad and unresolved apatite diffractions at about  $26^\circ$  and  $32^\circ$  in  $2\theta$  have been commonly interpreted as showing that such apatite was either poor in crystallinity or fine in grain size. Their FT-IR spectra had the carbonate ( $1500, 1417, \text{ and } 869 \text{ cm}^{-1}$ ) [22] bands, which confirmed that the carbonate ions were incorporated. Fig. 4 shows the typical morphology of the apatite layers covering the heated anatase-coating layer on the Ta substrates. The apatite layers with a similar microstructure were obtained for the Ti, NiTi and SUS 316L substrates, too. The smaller dots with  $< 1 \mu\text{m}$  in diameter in Fig. 4(a) were anatase. Fig. 4(b) shows that tiny spherical particles stacked and grown like linked beads; around the beads deposited were spherical apatite crystals with  $\sim 10 \mu\text{m}$  in diameter consisting of petal-like primary crystallites, but not on the beads. Such petal-like morphology is characteristic of apatite biomimetically deposited in SBF [4, 12, 14–16, 18–20]. Thus, the morphology of the samples was described as: the open spaces among the anatase beads aggregations were filled with apatite particles.

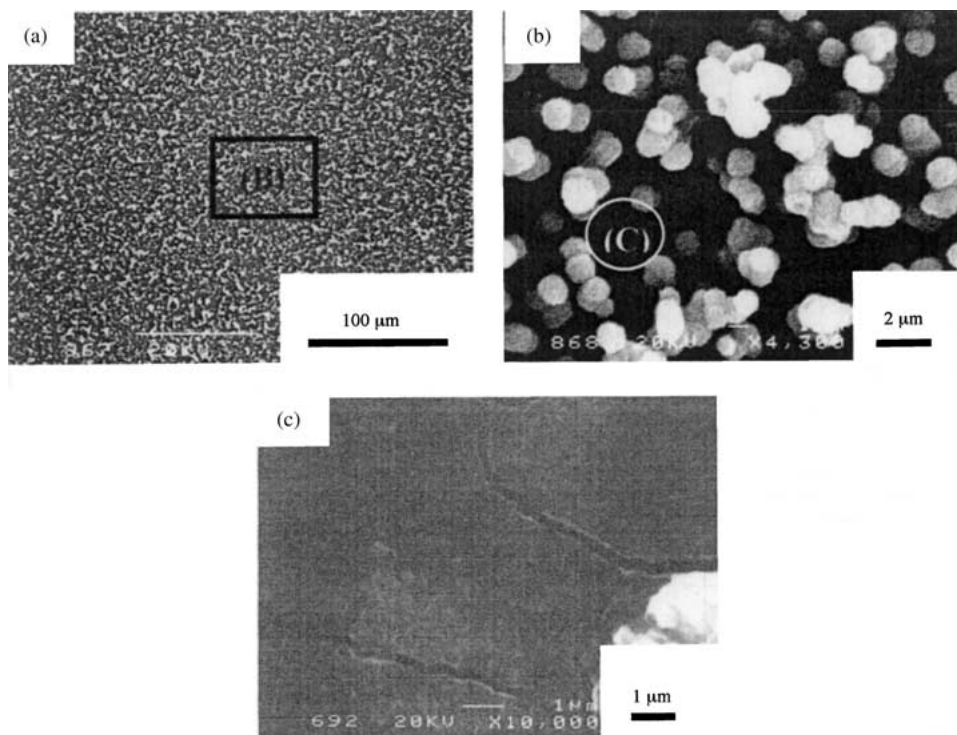


Figure 2 Dual layer morphology of the anatase layer coated on the Ta substrate. (a) The layer consisted of anatase particles; (b) a higher magnification image of (B) in (a); (c) a higher magnification image of the circled area (C) of (b), showing the denser anatase (An) layer with a few cracks beneath the anatase particle layer as well as agglomerated anatase particles.

Fig. 5 indicates the wide range XPS spectra of the anatase layers deposited on the Ti substrates. Here, spectrum (a) was for the as-coated Ti substrate and spectrum (b) was for the substrate heat-treated at 300 °C for 1 h. Note that spectrum (a) had the fluorine peak at

684.0 eV. Yet, after heating, the fluorine peak disappeared in spectrum (b). Fig. 6 showed the O1s XPS spectra, whose profiles were deconvoluted into three component peaks after Ohtsuki *et al.* [25]: the oxygen atoms in the surface oxide lattices (529.3 eV), in acidic Ti–OH groups and physisorbed H<sub>2</sub>O (530.8 eV), and in basic Ti–OH groups (532.1 eV). Although the heat treatment reduced remarkably the intensity of the peak for the –OH groups, there still remained in the film some –OH groups, especially the basic Ti–OH groups, which were believed to be responsible for the apatite nucleation and growth [25].

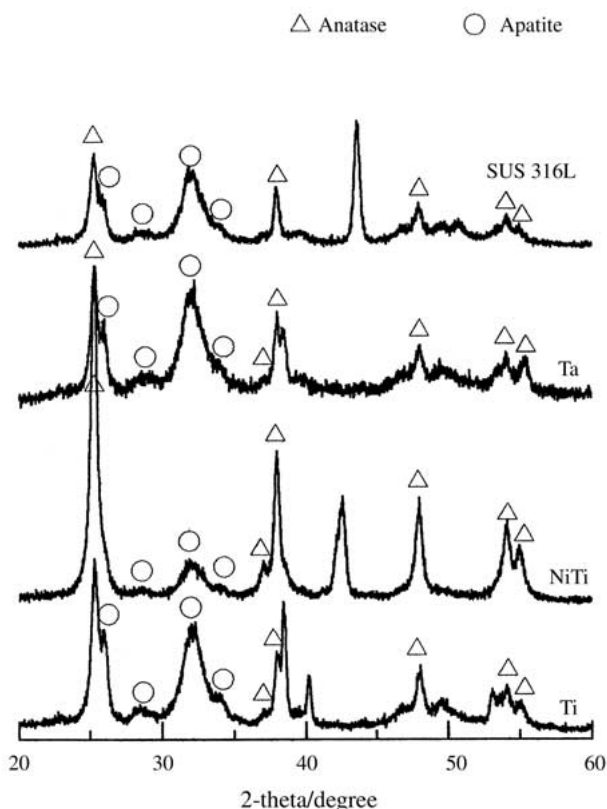
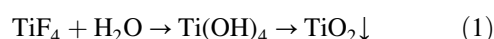


Figure 3 The TF-XRD patterns of the Ti, NiTi, Ta, and SUS316L substrates, treated with the TiF<sub>4</sub> solution, heated at 300 °C for 1 h, and subsequently soaked in SBF for 5 d (○: apatite, Δ: anatase). The diffractions without any symbols were from the substrates.

## 4. Discussion

### 4.1. Deposition of the anatase layer

In the sol–gel techniques, one of the most commonly used titanium resources is a group of titanium alkoxides (Ti(OR)<sub>4</sub>) [19, 20] such as titanium ethoxide (Ti(OEt)<sub>4</sub>) [21] and titanium isopropoxide (Ti(C<sub>3</sub>H<sub>7</sub>O)<sub>4</sub>) [22]. They are very sensitive to humidity and water as to be easily hydrolyzed and instantly precipitate amorphous titania. In contrast, TiF<sub>4</sub> is dissolvable in water under acidic conditions, and the solution is stable at ambient temperature due to the relatively strong Ti–F bonds [23]. With keeping the resulted transparent solution at 60 °C, hydrolysis (Equation 1) starts to form titania:



Thus, depositing titania changed the surface tint from silver to violet-blue due to the light interference as Gaul described [26]. Fig. 2 has indicated that the deposited titania layer gave the dual-layer microstructure: the solid bottom layer and the porous outer layer. It is commonly accepted that at earlier stages, the supersaturation of

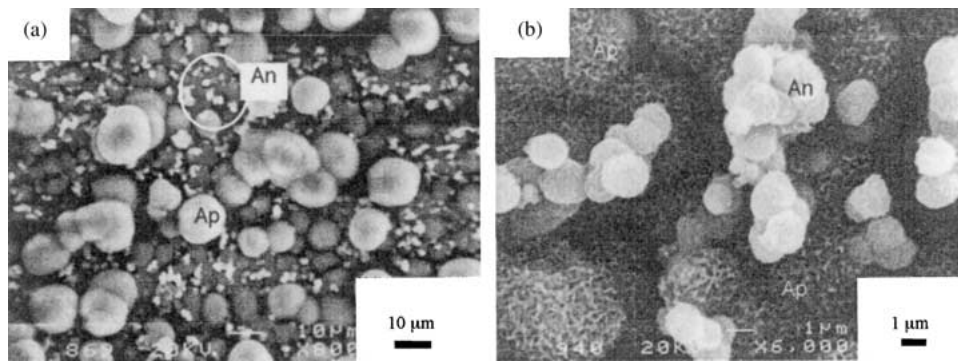


Figure 4 Surface morphology of the hydroxyapatite layer deposited on the anatase-coated Ta substrate. The larger spherical particles in (a) and spherical agglomerates of crystallites with a flake-like morphology in (b) were apatite (Ap). The white smaller dots in (a) and white spherical particles in (b) were anatase (An).

Ti(IV) is high and the formation of titania yields a layer on the substrates due to the high nucleation rate. At later stages with lower supersaturation, it is preferable for titania to be precipitated on the surface of the previously formed titania particles rather than to form new nuclei. Therefore, the titania deposition proceeded as illustrated in Fig. 7: (a) in the earlier stage, sub-nanometer-sized titania particles precipitated from the solution deposited on the substrate to form a homogeneous layer; and (b) at the later stage, titania deposited preferably on the surface of the previously grown titania particles, leading to a porous dual-layer surface structure.

The ordinary sol-gel procedure generally results in amorphous titania. Crystallization of the amorphous titania needs heating. However, the present process gave anatase under ambient conditions. Most trivial interpretation involves the equilibrium of dissolution and deposition of the titania yielded by the hydrolysis of  $TiF_4$  as well as structure relaxation leading to an ordered atomic arrangement. Here, important factors are moderate solubility of the titania gel and thermochemical stability of the Ti(IV) species in the  $TiF_4$  solution: too

large the rate of attachment of the incoming Ti(IV) species onto the growth sites might lend less time for them to form an ordered structure, and be likely to result in an amorphous structure. Thus, in other words, the fact that anatase has directly deposited on the substrates indicates that a moderate rate of polymerization and deposition is attained at the growing surface. The reduced rate is ascribed to the fluorine atoms in the surface layer as suggested by Shimizu *et al.* [23].

#### 4.2. Bioactivity of the anatase-coated substrates

Amorphous titania derived by any methods was not bioactive, but anatase obtained by heating it at appropriate temperatures was all found *in vitro* bioactive. The *in vitro* bioactivity is ascribed to Ti-OH groups or negatively charged surface as well as to an epitaxial effect of the anatase structure [12, 14, 18-20, 25].

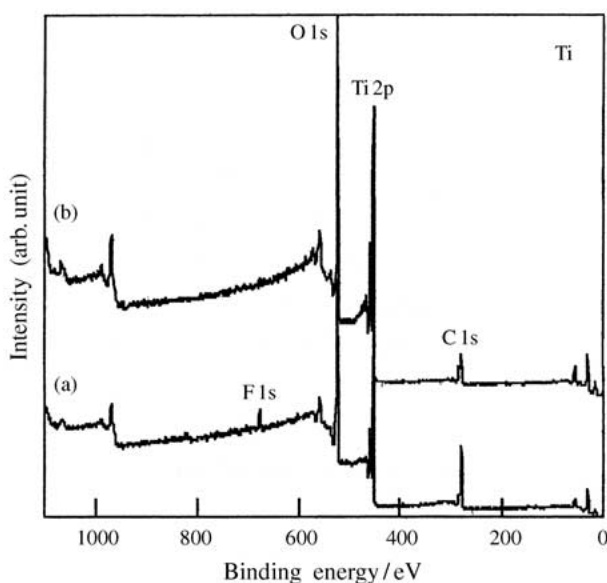


Figure 5 Wide-scan X-ray photoelectron spectra of the anatase layers deposited on the Ti substrate: (a) as-deposited, (b) after heating at 300 °C for 1 h in air. Note the presence of the F 1s peak at ~ 684.0 eV in (a) and the absence in (b).

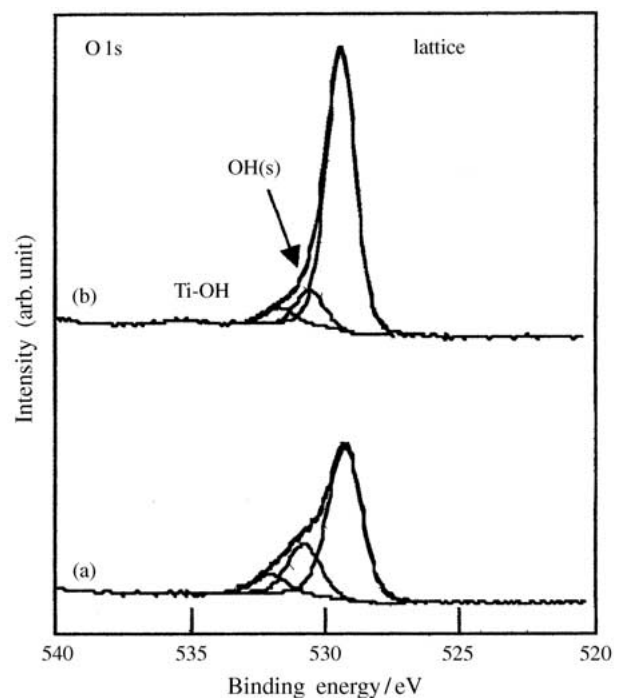


Figure 6 The X-ray photoelectron spectra of the O 1s core level for the anatase layers deposited on the Ti substrate: (a) as-deposited, (b) after heating at 300 °C for 1 h in air.

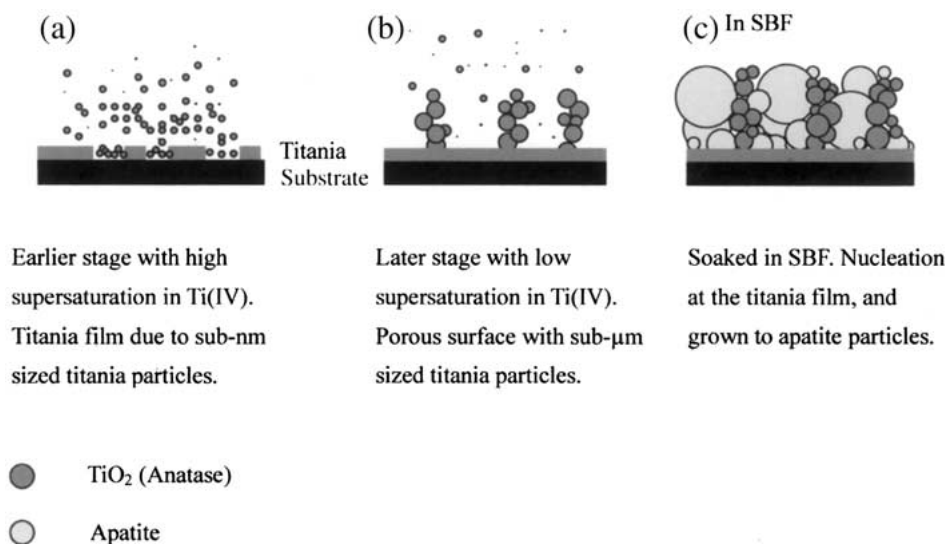


Figure 7 A schematic representation of anatase and apatite deposition on the metallic substrates. (a) In the earlier stages in the  $\text{TiF}_4$  solution; (b) in the later stages in the  $\text{TiF}_4$  solution; (c) after soaking in SBF.

However, the present experiment indicated that although anatase was precipitated directly from the  $\text{TiF}_4$  solution, the subsequent heat treatment at  $300^\circ\text{C}$  was necessary to induce apatite deposition within 5 d in SBF. After the XPS analysis in Fig. 5, the heat-treatment at  $300^\circ\text{C}$  eliminated fluorine from the anatase layer. Therefore, one cannot rule out the effects of the trace fluorine atoms incorporated in the anatase layers to depress significantly the apatite deposition. The binding energy of 684.0 eV for the F 1s core level in Fig. 5 is as large as that for ionic F in  $\text{CaF}_2$  (684.3 eV) [27] and smaller than that for covalent F in HF (687.0 eV [28]),  $\text{F}_2$ , and F–O bonds (687.4 eV [28, 29]). Thus, the fluorine atoms were present in the titania layers in an ionic state. It is speculated that they were attached on or loosely involved in the titania particles forming bonds like Ti–O–F, Ti–O–H–F and Ti–H–F since they were readily removed by heating at  $300^\circ\text{C}$ . Therefore, it is quite probable that when soaked in SBF the as-coated substrates would release the fluorine atoms into SBF. Those fluoride ions in SBF would reduce the activity of SBF to induce apatite nucleation, as Nakao *et al.* [30] pointed out.

The O 1s spectra in Fig. 6 have demonstrated that the basic Ti–OH groups remained in the anatase layer. Ohtsuki *et al.* [25] concluded that the basic Ti–OH groups favored the nucleation of apatite. Muñoz *et al.* [31] also confirmed the sol–gel-derived  $\text{TiO}_2$  to retain hydroxyls in its lattice even after the treatment at temperatures over  $600^\circ\text{C}$ . Thus, it is not strange that after eliminating the adverse effects of the fluorine atoms, all metallic substrates coated by the anatase layer induce apatite deposition in SBF within 5 d, according to the processes illustrated schematically in Fig. 7(c).

In conclusion, the present study has proposed a simple but versatile approach to provide various metallic biomaterials with the bioactive anatase layers. This method avoids the use of expensive equipments or high temperatures that encountered in the techniques such as plasma spraying and ion beam sputtering [7–10]. The method makes it unnecessary to use complicated and toxic reagents involved in the sol–gel methods [19, 20]. It is applicable to various metallic biomaterials with any

complex shapes. Therefore, the present process is quite promising as to contribute to both bioactive fixation of bone replacements and tissue engineering such as scaffolds for bone developments.

## 5. Conclusions

Well-crystallized anatase was deposited on the Ti, NiTi, Ta and SUS 316L substrates directly by soaking them in the 40 mM  $\text{TiF}_4$  solution at  $60^\circ\text{C}$  for 24 h. They had a dual-layer microstructure: the solid bottom layer and upper porous layer consisting of the linked-beads like agglomerated particles. The as-deposited anatase layers involved trace fluorine and could not deposit apatite in SBF within 10 d. When heated at  $300^\circ\text{C}$  for 1 h, the fluorine atoms were removed and the anatase layers deposited apatite in SBF within 5 d.

## Acknowledgments

Jin-Ming Wu gratefully acknowledges the financial support of the Venture Business Laboratories, the Graduate School of Natural Sciences, Okayama University. This work was performed when he was on leave from Zhejiang University, P. R. China. Partial financial supports by The Society of Non-Traditional Technology and Wesco Science Promotion Foundation are acknowledged.

## References

1. J. B. PARK and R. S. LAKES, in "Biomaterials: An Introduction", 2nd edn (Plenum Press, New York, 1992) p. 79.
2. C. P. SHARMA and W. PAUL, *J. Biomed. Mater. Res.* **26** (1992) 1179.
3. W. R. LACEFIELD, in "An Introduction to Bioceramics", edited by L. L. Hench and J. Wilson (World Scientific, Singapore, 1993) p. 223.
4. T. MIYAZAKI, H. M. KIM, F. MIYAJI, T. KOKUBO, H. KATO and T. NAKAMURA, *J. Biomed. Mater. Res.* **50** (2000) 35.
5. L. L. HENCH, *Biomaterials* **19** (1998) 1419.
6. K. TAKATSUKA, T. YAMAMURO, T. NAKAMURA and T. KOKUBO, *J. Biomed. Mater. Res.* **29** (1995) 157.

7. J. WENG, Q. LIU, J. G. C. WOLKE, X. D. ZHANG and K. DE GROOT, *Biomaterials* **18** (1997) 1027.
8. D. R. BLOYER, J. M. GOMEZ-VA, E. SAIZ, J. M. MCNANEY, R. M. CANNON and A. P. TOMSIA, *Acta. Mater.* **47** (1999) 4221.
9. X. Y. LIU, C. X. DING and Z. Y. WANG, *Biomaterials* **22** (2001) 2007.
10. H. ZENG, K. K. CHITUR and W. R. LACEFIELD, *ibid.* **20** (1999) 443.
11. J. W. M. VEHOF, P. H. M. SPAUWEN and J. A. JANSEN, *ibid.* **21** (2000) 2003.
12. H. M. KIM, F. MIYAJI, T. KOKUBO and A. NAKAMURA, *J. Biomed. Mater. Res.* **32** (1996) 409.
13. M. WEI, A. J. MILTHORPE, C. C. SORRELL and J. H. EVANS, *J. Sol-Gel Sci. Techn.* **21** (2001) 39.
14. X. X. WANG, S. HAYAKAWA, K. TSURU and A. OSAKA, *J. Biomed. Mater. Res.* **52** (2000) 171.
15. T. MIYAZAKI, H. M. KIM, F. MIYAJI, T. KOKUBO, H. KATO and T. NAKAMURA, *ibid.* **50** (2000) 35.
16. T. MIYAZAKI, H. M. KIM, F. MIYAJI, T. KOKUBO, H. KATO and T. NAKAMURA, *J. Mater. Sci.: Mater. Med.* **12** (2001) 683.
17. H. M. KIM, T. MIYAZAKI, T. KOKUBO and T. NAKAMURA, in "Bioceramics 13", edited by S. Giannini and A. Moroni (Trans. Tech. Publications Ltd, Switzerland, 2001) p. 47.
18. M. UCHIDA, H. M. KIM, T. KOKUBO and T. NAKAMURA, in "Bioceramics 12", edited by H. Ohgushi, G. W. Hastings and T. Yoshikawa (World Scientific, NJ, 1999) p. 149.
19. P. J. LI, I. KANGASNIEMI, K. DE GROOT and T. KOKUBO, *J. Am. Ceram. Soc.* **77** (1994) 1307.
20. T. PELTOLA, M. PATSI, H. RAHALA, I. KANGASNIEMI and A. YLI-URPO, *J. Biomed. Mater. Res.* **41** (1998) 504.
21. J. L. KEDDIE, P. V. BRAUN and E. P. GIANNELIS, *J. Am. Ceram. Soc.* **77** (1994) 1592.
22. Y. TAKAHASHI, A. OHSUGI, T. ARAFUKA, T. OHYA, T. BANAND and Y. OHYA, *J. Sol-Gel Sci. Techn.* **17** (2000) 227.
23. K. SHIMIZU, H. IMAI, H. HIRASHIMA and K. TSUKUMA, *Thin Solid Films* **351** (1999) 220.
24. U. POSSET, E. LOCKLIN, R. THULL and W. KIEFER, *J. Biomed. Mater. Res.* **40** (1998) 640.
25. C. OHTSUKI, H. IIDA, S. HAYAKAWA and A. OSAKA, *ibid.* **35** (1997) 39.
26. E. GAUL, *J. Chem. Edu.* **70** (1993) 176.
27. S. HAYAKAWA, A. NAKAO, C. OHTSUKI, A. OSAKA, S. MATSUMOTO and Y. MIURA, *J. Mater. Res.* **13** (1998) 739.
28. Y. SAITO and Y. NAKAZAWA, *J. Appl. Phys. Jpn.* **36** (1997) 1466.
29. K. NINOMIYA, K. SUZUKI, S. NISHIATSU and O. OKADA, *J. Appl. Phys.* **58** (1985) 1177.
30. A. NAKAO, K. TSURU, S. HAYAKAWA, C. OHTSUKI and A. OSAKA, in "Bioceramics 9", edited by T. Kokubo, T. Nakamura and F. Miyaji (Cambridge University Press, Cambridge, 1996) p. 131.
31. E. MUÑOZ, J. L. BOLDÚ, E. ANDRADE, O. NOVARO, X. BOKHIMI, T. LÓPEZ and R. GÓMEZ, *J. Am. Ceram. Soc.* **84** (2001) 392.

*Received 26 March  
and accepted 3 April 2003*